15

Terahertz frequency metrology based on frequency comb techniques

T. YASUI, Osaka University, Japan

DOI: 10.1533/9780857096494.2.436

Abstract: For a long time there has been a gap in frequency metrology in the terahertz (THz) region of the spectrum, between the optical and electrical regions, due to the lack of a frequency standard and traceability in this region. This chapter describes the concept of a new THz frequency metrology method based on a frequency comb, which is designed to fill this gap. Three techniques embodying the concept are also described: a THz-comb-referenced spectrum analyzer, an optical-comb-referenced THz synthesizer and a THz-comb-referenced spectrometer. Via coherent frequency linking among microwave, optical and THz waves, these three techniques are traceable to a microwave frequency standard and hence possess the same frequency uncertainty as that in the optical and electrical regions. Traceability of these techniques to the microwave frequency standard will ensure reliability of the frequency scale in the THz spectrum, which will expand the scope of various THz applications.

Key words: frequency metrology, traceability, optical comb, THz comb, photoconductive mixing.

15.1 Introduction

Terahertz (THz) electromagnetic waves, lying at the boundary between optical and electrical waves, have emerged as a new mode for sensing, spectroscopy, communication and other applications (Mittleman, 2003; Tonouchi, 2007). Along with recent progress in THz technology and science, the requirements of THz metrology have increased in various applications of THz photonics because metrology is an important technical infrastructure guaranteeing reliability of measurement in industry (Kleine-Ostmann *et al.*, 2008; Yasui *et al.*, 2011a). In particular, frequency is an important quantity to be measured in THz metrology because it is a fundamental physical quantity of electromagnetic waves. In contrast to electrical and optical regions, reliable frequency metrology has not yet been established in the THz region, due to the fact that source and detector technologies are still immature in this frequency region. Such a 'THz gap' in frequency metrology

could hinder the growth of various THz applications. If reliable THz frequency metrology could be established based on the national frequency standard, the scope of THz applications would be greatly expanded as a result of the high reliability achieved.

An ideal approach for establishing reliable THz frequency metrology is to use a transition frequency in an atom for a frequency standard. For example, a frequency standard at 9.2 GHz was established based on the hyperfine transition in the cesium atom, which is the basis of the definition of time in the International System of Units (SI). In the THz region, a scheme for establishing a frequency standard based on three-photon coherent population trapping in stored ions has been proposed (Champenois *et al.*, 2007); however, realizing this scheme will be challenging in practice. Another practical approach for frequency metrology is to transfer the frequency uncertainty of other electromagnetic-wave regions, where reliable frequency standards have already been established, to the THz region. To achieve this, frequency linking between two electromagnetic-wave regions is required. Recently, an optical frequency comb was used to distribute the frequency uncertainty of a microwave frequency standard to the optical region directly (Udem *et al.*, 2002). Furthermore, the concept of a frequency comb has been extended to the THz region (Yasui *et al.*, 2006). These techniques show promise for realizing reliable frequency metrology in the THz region.

In this chapter, three techniques for THz frequency metrology based on a frequency comb are reviewed. Coherent frequency linking among the microwave, optical and THz regions, achieved by frequency comb techniques, is described in Section 15.2. A THz-comb-referenced spectrum analyzer for precise frequency measurement of continuous-wave (CW) THz waves is presented in Section 15.3. Section 15.4 describes the demonstration of an optical-comb-referenced THz synthesizer using photomixing of two optical frequency synthesizers phase-locked to a microwave frequency standard. In Section 15.5, a THz-comb-referenced spectrometer is described, in which each mode of the THz comb is used as a frequency marker for a broadband THz spectrum. Section 15.6 summarizes our work and discusses some goals for future research.

15.2 Coherent frequency linking with frequency comb

Figure 15.1 illustrates the principles of an optical comb and a THz comb in the time and frequency domains. A femtosecond mode-locked (fs-ML) laser generates a sequence of pulses that are essentially copies of the same pulse separated by an interval equal to the inverse of the mode-locked

frequency, f_{rep} (Yasui *et al.*, 2011a). The highly stable fs-ML pulse train is synthesized by a series of regular frequency spikes separated by f_{rep} in the optical frequency domain. This structure is referred to as a frequency comb. Since the frequency comb structure can be used as a precision frequency ruler in the optical region, the fs-ML-laser-based optical frequency comb has received a lot of interest as a powerful metrological tool capable of covering the optical region by virtue of precise laser stabilization (Udem *et al.*, 2002). Recently, the concept of the frequency comb has been extended to the THz region by combining fs-ML pulse trains with a photoconductive process (Yasui *et al.*, 2006). When a photoconductive antenna (PCA) for THz generation is irradiated by the fs-ML optical pulse train, a free-space-propagating, mode-locked THz pulse train is radiated from the PCA. This THz pulse train is composed of a regular comb of sharp lines of electromagnetic waves in the THz frequency domain, namely, an electromagnetic THz comb (EM-THz comb). On the other hand, when the fs-ML optical pulse train is incident on a PCA used for THz detection, the instantaneous generation of photocarriers is repeated in the PCA in synchronization with the optical pulse train. The resulting mode-locked THz pulse train of photocarriers constructs a frequency comb structure of photocarriers in the THz region, namely, a photocarrier THz comb (PC-THz comb). In this way, the optical comb is down-converted to the THz region without any change in its frequency spacing. The resulting THz comb is a harmonic frequency comb without any frequency offset, composed of a fundamental component and a series of harmonic components of the mode-locked frequency f_{rep}. This is the biggest difference compared with an optical frequency comb having a carrier-envelope offset frequency (f_{ceo}), which has to be stabilized. Since the optical comb and THz comb are considered to be a set of several thousand or several tens of thousands of narrow-linewidth, single-mode CW waves, they provide attractive features for frequency metrology, such as simplicity, broadband selectivity, high spectral purity and absolute frequency calibration. Therefore, if f_{rep} and f_{ceo} can be well stabilized by laser control, the optical and THz combs can be used as precise frequency rulers in the optical and THz regions, respectively.

Figure 15.2 shows the concept of THz frequency metrology based on the frequency comb. Atomic clocks in the microwave region have been widely used as standards of time and frequency. However, it has been difficult to transfer the frequency uncertainty of the atomic clocks to the optical region due to the large frequency gap between the microwave and optical regions. Although such a gap has been bridged by a frequency chain (Schnatz *et al.*, 1996), it is a rather bulky and complicated apparatus. Furthermore, the frequency uncertainty deteriorates while passing through many intermediate oscillators in the chain. Recently, an optical comb has emerged as a powerful tool for frequency linking between the microwave and optical regions

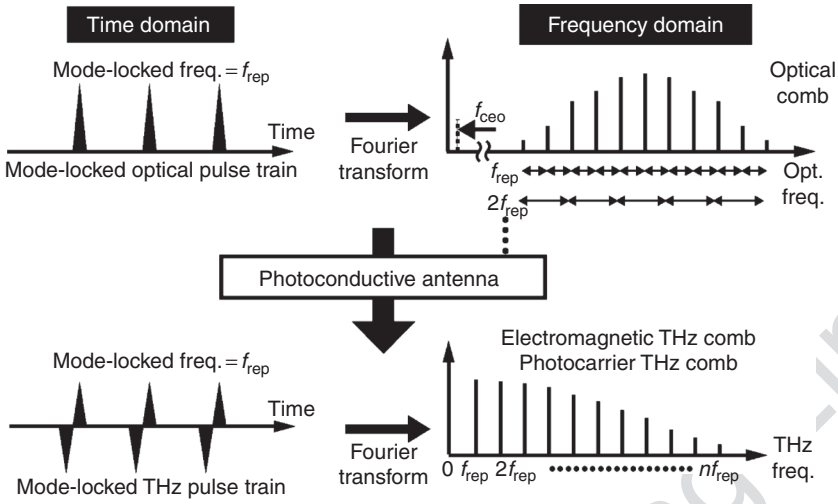

15.1 Optical comb and THz comb.

directly, without losing the frequency uncertainty, by achieving precise laser stabilization with an atomic clock (Udem *et al.*, 2002). Furthermore, the frequency comb has been extended to the THz region using a PCA, as shown in Fig. 15.1 (Yasui *et al.*, 2006). Here, the most important point is that frequency linking among the microwave, optical and THz regions is based on a coherent process, involving laser control and a photoconductive antenna. The resulting coherent frequency linking enables us to share the same frequency uncertainty in three different regions of the electromagnetic spectrum. Therefore, based on a THz comb or optical comb, one can construct a THz frequency metrology system that is directly connected to a frequency standard in the microwave region. In other words, THz frequency metrology traceable to the SI base unit of time can be established.

15.3 Terahertz (THz)-comb-referenced spectrum analyzer

A spectrum analyzer is a fundamental frequency measurement instrument widely used for radio frequency (RF), microwave and millimeter waves. However, it is still difficult to use in the THz region, although steady efforts are being made to extend its frequency range. The electrical heterodyne method with a superconductor-insulator-superconductor mixer (Kohjiro *et al.*, 2008) or a hot-electron-bolometer mixer (Baselmans *et al.*, 2004) enables frequency measurement of CW waves in the sub-THz and THz regions. Conversely, the optical interferometric method can be used

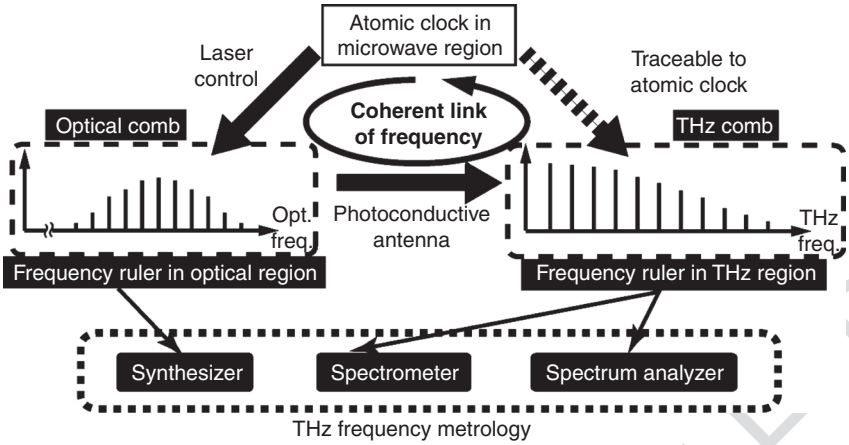

15.2 Coherent link of frequency using frequency comb.

as an optical spectrum analyzer in the THz region. However, those methods often require cryogenic cooling of the mixer or detector to suppress thermal noise, which is a major obstacle to practical use. Recently, a new type of spectrum analyzer based on a harmonic mixing technique with a frequency comb has been proposed and developed. This device can measure the absolute frequency and spectral shape of CW-THz waves in real time without the need for cryogenic cooling (Yokoyama *et al.*, 2008; Yasui *et al.*, 2009).

15.3.1 Principle of operation

In the field of microwave technology, harmonic mixing technique based on electro-optic sampling has been often used to down-convert microwave spectrum to RF spectrum using the comb spectrum of the mode-locked laser with a nonlinear detection technique (Kolner and Bloom, 1986; Gopalakrishnan *et al.*, 1993). Furthermore, this technique has been extended to the THz region (Gaal *et al.*, 2007). We here modified this technique to down-convert THz spectrum to RF spectrum using photoconductive detection. Our THz spectrum analyzer is based on a heterodyne technique as shown in Fig. 15.3a. In this heterodyne method, the PC-THz comb is used as an RF signal with multiple frequencies covering from the sub-THz to THz regions, whereas a measured CW-THz wave works as a local oscillator. Since each mode of THz comb has a low power, the moderate power is required for the measured CW-THz wave to get the beat signal at good signal-to-noise ratio (Yokoyama *et al.*, 2008; Yasui *et al.*, 2009). Moreover, combining terahertz PCAs and PC-THz combs enables

AQ1

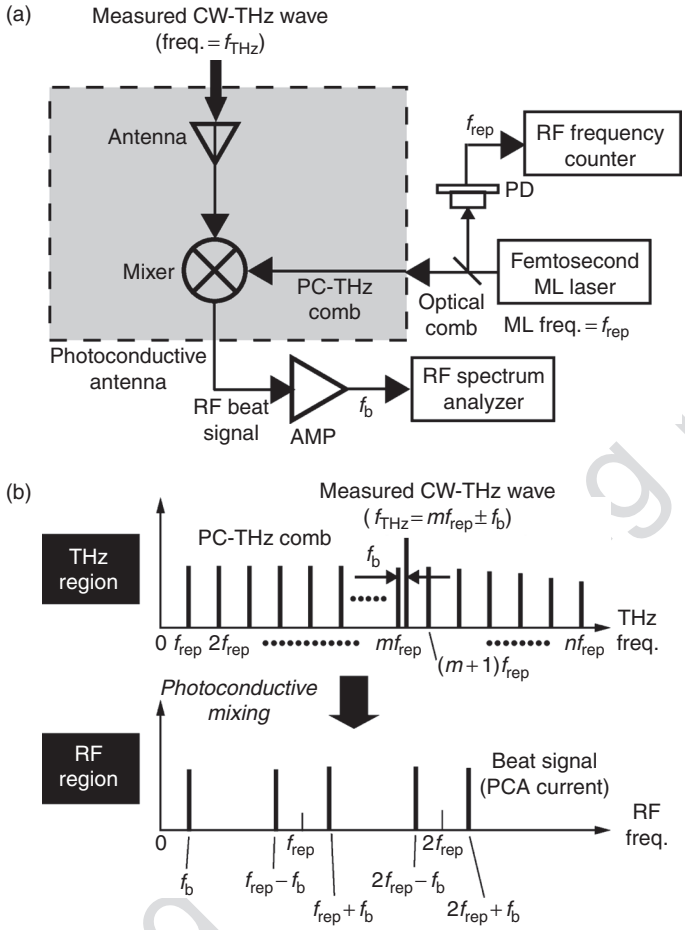

15.3 (a) Principle of THz-comb-referenced spectrum analyzer and (b) the corresponding spectral behavior in THz and RF regions.

heterodyne mixing covering from the sub-THz to THz regions without the need for cryogenic cooling.

Consider a PCA detector triggered by an fs-ML laser beam with repetition frequency f_{rep}. Figure 15.3b illustrates the corresponding spectral behaviors in THz and RF regions. The probe pulse train emitted from the fs-ML laser constructs an optical frequency comb in the frequency domain, whose mode spacing is equal to a mode-locked frequency (see Fig. 15.1). When the PCA is triggered by such pulse train, the PC-THz comb is induced in the PCA. Next, consider what happens when a measured CW-THz wave (frequency = f_{THz}) is incident on a PCA detector triggered by the probe pulse train. The photoconductive mixing process in the PCA generates a group of

beat signals between the CW-THz wave and the PC-THz comb in the RF region. Focus on a beat signal at the lowest frequency (= f_b), namely f_b beat signal. Since this f_b beat signal is generated by mixing the CW-THz wave (frequency = f_{THz}) with the m$^{\mathrm{th}}$ mode of the PC-THz comb (frequency = mf_{rep}) nearest in frequency to the CW-THz wave, f_{THz} is given as follows:

$$f_{\mathrm{THz}} = mf_{\mathrm{rep}} \pm f_b. \qquad [15.1]$$

Since f_{rep} and f_b can be measured by RF frequency instruments, f_{THz} can be determined if the value of m and the sign of f_b are measured. To this end, the mode-locked frequency is changed from f_{rep} to $f_{\mathrm{rep}} + \delta f_{\mathrm{rep}}$ by adjustment of the laser cavity length with the laser control system. This results in a change of the beat frequency to $f_b + \delta f_b$. Since $|\delta f_b|$ is equal to $|m\delta f_{\mathrm{rep}}|$, the value of m is determined as:

$$m = \frac{|\delta f_b|}{|\delta f_{\mathrm{rep}}|}. \qquad [15.2]$$

and $\delta f_b/\delta f_{\mathrm{rep}}$ and f_b have opposite signs. Finally, the absolute frequency of the measured CW-THz wave can be determined by measuring f_{rep}, f_b, δf_{rep} and δf_b because

$$f_{\mathrm{Thz}} = mf_{\mathrm{rep}} + f_b\left(\frac{\delta fb}{\delta f_{\mathrm{rep}}} < 0\right) \qquad [15.3a]$$

and

$$f_{\mathrm{THz}} = mf_{\mathrm{rep}} - f_b\left(\frac{\delta f_b}{\delta f_{\mathrm{rep}}} > 0\right). \qquad [15.3b]$$

15.3.2 Experimental set-up

Figure 15.4 shows a schematic diagram of the experimental set-up. The THz-comb-referenced spectrum analyzer was composed of a home-built, fs-ML Er-doped fiber laser (center wavelength = 1550 nm, pulse duration = 40 fs and f_{rep} = 56 122 206 Hz) (Inaba *et al.*, 2006), a PCA for THz detection and RF frequency instruments. The mode-locked frequency f_{rep} was stabilized using a laser control system referenced to a rubidium (Rb) atomic clock (Stanford Research Systems FS725 with frequency = 10 MHz, accuracy = 5

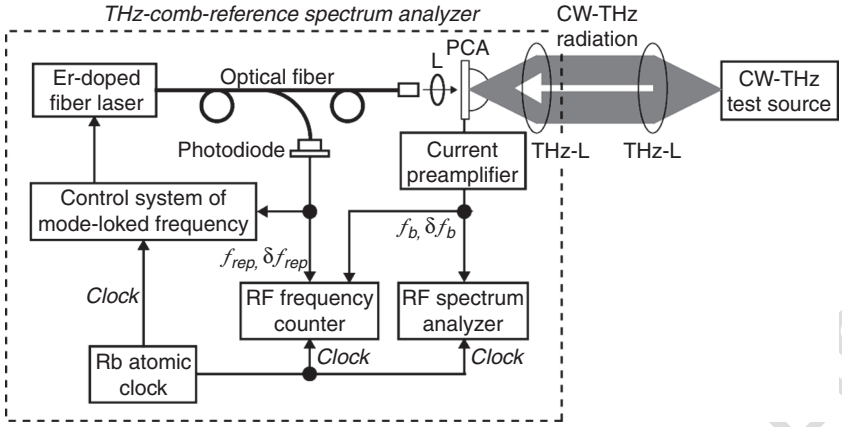

15.4 Experimental set-up of THz-comb-referenced spectrum analyzer. L: lens; PCA: bowtie-shaped, low-temperature-grown InGaAs/InAlAs photoconductive antenna; THz-L: THz lenses.

× 10–11, stability = 2 × 10–11 at 1 s). The output of the fiber laser was delivered to a bowtie-shaped, low-temperature-grown InGaAs/InAlAs PCA for a 1550 nm laser light (Menlo Systems GmbH, BT10) by an optical fiber. This results in generation of the PC-THz comb in the PCA equivalent to the Rb atomic clock. The CW-THz wave from a test source propagated in free space through a pair of THz lens (Pax Co., Tsurupica), and was then incident on the PCA. Photoconductive heterodyne mixing between the CW-THz wave and the PC-THz comb in the PCA generates a group of beat signals in the RF region. The f_b beat signal is amplified by a high-gain current preamplifier (bandwidth = 10 MHz and sensitivity = 10^5 V/A) and was measured with an RF spectrum analyzer (Agilent E4402B with a frequency range of 100 Hz to 3 GHz) and an RF frequency counter (Agilent 53132A with a frequency range to 225 MHz) to determine its spectral shape and center frequency. A portion of the laser light is detected with a photodetector, and its mode-locked frequency (= f_{rep}) is measured using the RF frequency counter. The RF spectrum analyzer and RF frequency counter are synchronized to the Rb atomic clock.

15.3.3 Results

The first test source (output power = 4 dBm = 2.5 mW, frequency range = 75–110 GHz and linewidth < 0.6 Hz) is achieved by combination of an active frequency multiplier chain (Millitech AMC-10-R0000 with multiplication factor = 6) and a microwave frequency synthesizer (Agilent E8257D with frequency = 12.5–18.33 GHz), referred to as an AFMC source. Since

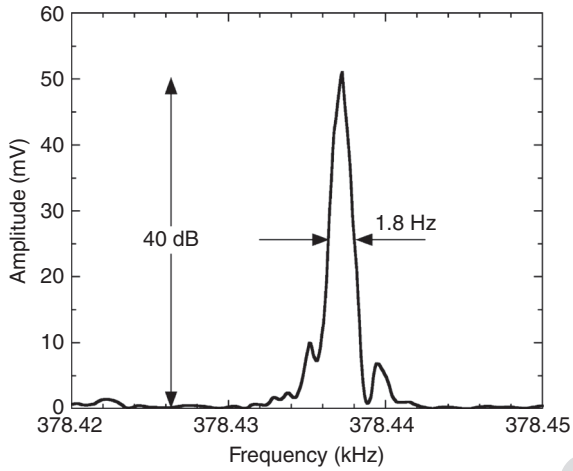

15.5 Spectra of the f_b beat signal of the AFMC source measured by the RF spectrum analyzer (RBW = 1 Hz and sweep time = 690 ms).

the frequency synthesizer is synchronized to the Rb atomic clock, output frequency of this AFMC source is accurate and stable. We first evaluated the spectral linewidth of the f_b beat signal when the output frequency of the AFMC source was set to 100 GHz. Figure 15.5 shows a linear-scale spectrum of this signal, measured by the RF spectrum analyzer (resolution bandwidth (RBW) = 1 Hz and sweep time = 690 ms). The resulting linewidth of the beat signal was 1.8 Hz. This result indicates that each mode of the PC-THz comb has sufficiently narrow linewidth to perform the frequency measurement with high precision. On the other hand, the signal-to-noise ratio (SNR) of the f_b beat signal reached 40 dB. From this SNR and the output power of the test source (namely + 4 dBm = 2.5 mW), the detection limit of the THz power is estimated to –36 dBm, or 250 nW. Comparison of SNR among the f_b beat signals obtained by three different PCAs and electro-optic sampling is given in detail elsewhere (Yasui *et al.*, 2009).

To determine the absolute frequency of the test source, it is necessary to measure the deviation of f_b before and after changing f_{rep}. The initial f_{rep} and f_b values were measured to be 56 122 206.03 Hz and 356 156 Hz as indicated as the left spectrum in Fig. 15.6 (RBW = 1 kHz and sweep time = 902 ms). Then, the frequency f_{rep} was changed by δf_{rep} (= +25 Hz) using the laser control system. This resulted in a change of the beat frequency by δf_b of 44 549 Hz (see the right spectrum in Fig. 15.6). Since $|\delta f_b|$ is equal to $|m\delta f_{\text{rep}}|$, m is determined as

$$m = \frac{|\delta f_b|}{|\delta f_{\text{rep}}|} = \frac{|+44,549|}{|+25|} = 1,781.96 \approx 1,782. \qquad [15.4]$$

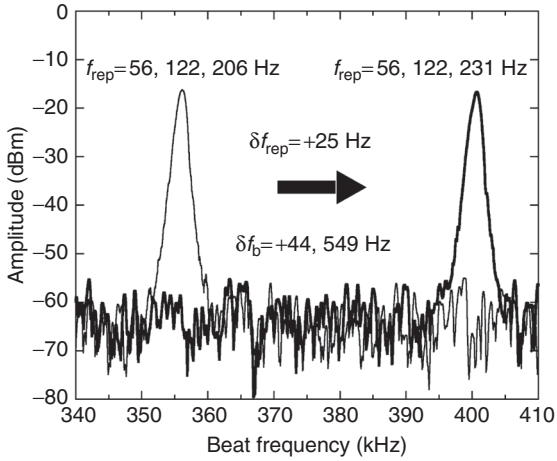

15.6 Experimental set-up. SHG: second-harmonic-generation crystal; L: lenses; PCA1 and PCA2: dipole-shaped LTG-GaAs photoconductive antennas; Si-L: hemispherical silicon lenses; THz-L: THz lenses; AMP: current preamplifier.

Since the sign of $\delta f_b/\delta f_{\text{rep}}$ (positive in this case) is opposite to that of f_b, the value of f_{THz} was determined as follows:

$$f_{\text{THz}} = mf_{\text{rep}} - f_b = 1,782 * 56,122,206.03 - 356,156 = 100,009414,989.46 \text{ Hz}. \quad [15.5]$$

Since the actual set frequency of the AFMC source was 100 009 414 988.9 Hz from the output frequency of the microwave synthesizer, the error between the set and measured frequencies was only 0.56 Hz. When precision of frequency measurement is defined as the ratio of the error to f_{THz}, the corresponding precision was 5.6×10^{-12}.

To evaluate the precision of frequency measurement in available frequency range of the AFMC source, we determined the absolute frequency of the source while tuning its output frequency from 75 to 110 GHz at 5 GHz intervals. The resulting precision for eight different measurement frequencies is shown in Fig. 15.7, in which the precision is defined as a ratio of the frequency error to the set frequency of the test source, A mean precision of 2.4×10^{-11} was obtained for this source, which is limited by the performance of the Rb atomic clock used. The frequency precision will be further improved if we use a frequency standard having less uncertainty, such as cesium atomic clock.

The second test source was produced by photomixing of two CW near-infrared lasers at adjacent wavelengths with a uni-traveling-carrier photodiode (UTC-PD) (Nagatsuma *et al.*, 2009). The two CW lasers were external cavity wavelength-tunable laser diodes with an emission wavelength of 1550

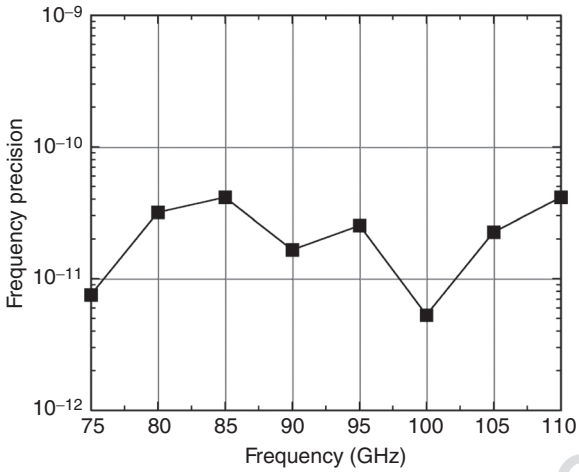

15.7 Precision of frequency measurement in available frequency range of the AFMC source.

nm and operated in free-running mode (Koshin Kogaku Co., LS-601A-15S1; spectral linewidth ≤ 100 kHz, frequency fluctuation < 100 MHz/h). The optical frequency difference between them was set to be approximately 120 GHz. The outputs of the lasers were combined using a fiber coupler, amplified with an Er-doped fiber amplifier, and then photomixed by an F-band UTC-PD (NTT Electronics, available frequency = 90–140 GHz) equipped with a horn antenna. The output power was set to be 100 μW at a frequency of 120 GHz. We used the THz-comb-referenced spectrum analyzer for monitoring this photomixing source. The resulting spectrum of the beat signal is shown in Fig. 15.8 (RBW = 1 kHz, sweep time = 13 ms). The detailed spectral behavior of the beat signals is shown as a video elsewhere (Yasui *et al.*, 2009). In contrast to the stable AFMC source, the beat frequency of the photomixing source exhibits large fluctuations within a spectral window of 0.8 MHz. This is because the two CW lasers used for the photomixing are operating in free-running mode without any frequency control.

Although the frequencies of the above test sources were in the low-frequency THz region due to the limitation of our available CW-THz sources, it is natural to believe that this THz spectrum analyzer can be extended to the higher frequency THz region. This is because the spectral bandwidth of the THz spectrum analyzer is limited mainly by spectral sensitivity of the PCA. For example, the spectral characteristics of the LT-GaAs-PCA as a THz detector have been investigated using THz time-domain spectroscopy (THz-TDS), for which a bandwidth over 100 THz was achieved (Katayama *et al.*, 2010). Therefore, the THz-comb-referenced spectrum analyzer can cover the entire THz spectral region.

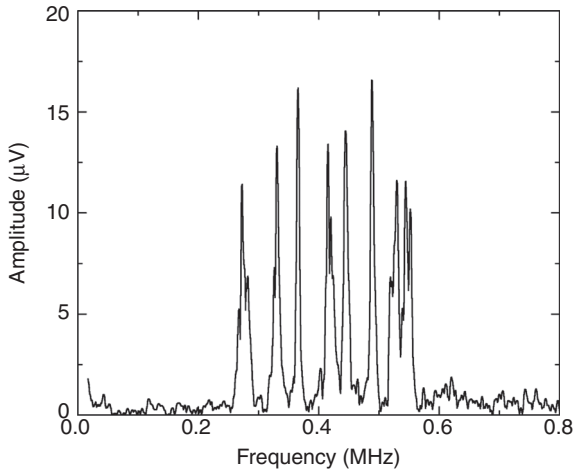

15.8 Spectrum of the f_b beat signal of the photomixing source (RBW = 1 kHz and sweep time = 13 ms).

15.4 Optical-comb-referenced THz synthesizer

Accurate, stable and/or tunable single-frequency signal generation is an essential technique in developing the THz clock and synthesizer. One promising method for widely tunable CW-THz sources is photomixing two CW near-infrared lasers of adjacent wavelengths with a photomixer, such UTC-PD (Nagatsuma *et al.*, 2009) or PCA (Matsuura *et al.*, 1997). However, if the two CW lasers are operated in the free-running mode, it is difficult to generate an accurate and stable frequency in the CW-THz wave as shown in Fig. 15.8. One attractive frequency reference for simultaneous control of these two CW lasers is an optical frequency comb (Udem *et al.*, 2002). An accurate, stable, phase-locked CW-THz wave has been discretely generated at four different frequencies (0.30, 0.56, 0.84 and 1.1 THz) by photomixing of two CW lasers locked to a single optical comb based on a mode-locked Ti: Sapphire laser (Quraishi *et al.*, 2005). Furthermore, the output frequency was tuned continuously by scanning the frequency interval of the optical comb while locking the CW lasers to the comb; however, the range of continuous tuning was limited to several kilohertz. In the case where the two CW lasers share the same optical comb, when scanning the frequency interval of the comb the optical frequencies of the two CW lasers change simultaneously. This common-mode change cancels most of the optical frequency change in the two CW lasers. As a result, the continuous tuning range of the CW-THz wave is much smaller than that of the optical frequency in the CW lasers. One promising approach to increase the continuous tuning range

while maintaining excellent frequency uncertainty is photomixing two independent optical frequency synthesizers (OFS) phase-locked to a microwave frequency standard (Yasui *et al.*, 2010b, 2011b).

15.4.1 Principle of operation

An OFS is realized by phase-locking a tunable single-frequency CW laser to one of the optical comb modes (Takahashi *et al.*, 2009). When the frequency spacing and carrier-envelope-offset frequency in the optical comb and the beat frequency between the CW laser and one of the comb modes are fully phase-locked to the microwave frequency standard, the optical frequency of the OFS can be determined at the uncertainty of the frequency standard via the optical comb. Furthermore, the optical frequency can be widely and continuously tuned by scanning the comb spacing while maintaining the phase-locking. Therefore, if the outputs from a tunable OFS and a fixed frequency OFC are optically heterodyned with a photomixer, the generated CW-THz radiation is widely and continuously tunable while its frequency is always determined, referenced to the microwave frequency standard.

Let us consider the optical frequency f_{ofs1} of a fixed OFS (OFS1), composed of a CW laser (CWL1) and a fiber-based optical comb (FC1), as shown in the upper part of Fig. 15.9. The optical frequency f_{ofs1} is represented by (Takahashi *et al.*, 2009)

$$f_{\mathrm{ofs1}} = f_{\mathrm{ceo1}} + m_1 f_{\mathrm{rep1}} + f_{\mathrm{beat1}}, \qquad [15.6]$$

where f_{ceo1} and f_{rep1} are the carrier-envelope offset frequency and repetition rate of FC1, respectively, m_1 is the mode number of the comb to which CWL1 is phase-locked, and f_{beat1} is the beat frequency between CWL1 and the $m_1{}^{\mathrm{th}}$ mode. In the fixed OFS, f_{ceo}, f_{rep1}, m_1 and f_{beat1} are all stabilized at fixed values by precise laser control referenced to a microwave frequency standard. Therefore, f_{ofs1} can be determined at the uncertainty of the optical comb.

On the other hand, the optical frequency f_{ofs2} of a tunable OFS (OFS2), composed of another CW laser (CWL2) and another fiber comb (FC2), as shown in the lower part of Fig. 15.9, is given by

$$f_{\mathrm{ofs2}} = f_{\mathrm{ceo2}} + m_2 f_{\mathrm{rep2}} + f_{\mathrm{beat2}}, \qquad [15.7]$$

where f_{ceo2} and f_{rep2} are the carrier-envelope offset frequency and repetition rate of FC2, respectively, m_2 is the mode number of the comb to which CWL2 is phase-locked, and f_{beat2} is the beat frequency between CWL2 and

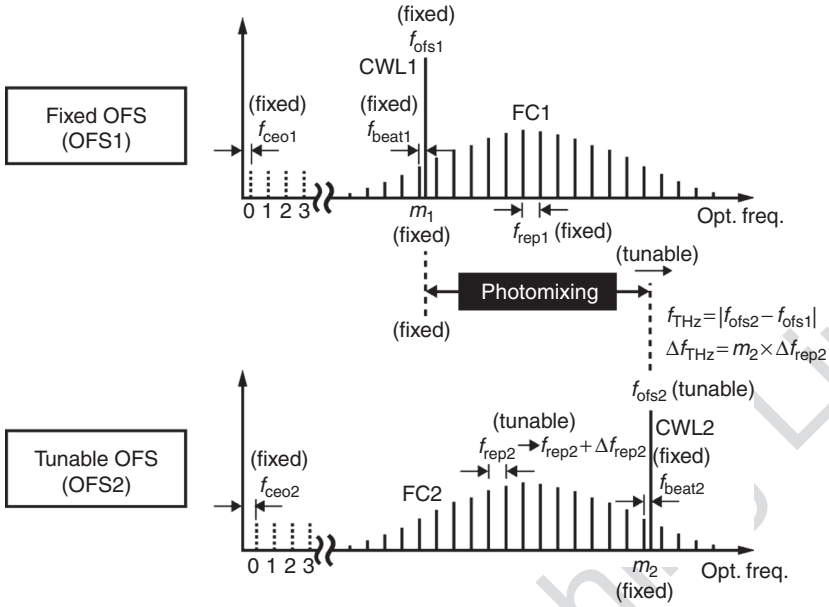

15.9 Principle of THz synthesizer based on photomixing of two OFSs.

the m_2^{th} mode. If the comb spacing is changed from f_{rep2} to $f_{rep2} + \Delta f_{rep2}$ while keeping f_{ceo2} at a fixed value, all the modes of FC2 expand in a manner similar to the bellows of an accordion, and thus the frequency of the m_2^{th} mode changes by the product of m_2 and Δf_{rep2}. Therefore, f_{ofs2} can also be tuned continuously by $m_2 \Delta f_{rep2}$ if CWL2 remains phase-locked to the m_2-th comb mode. In the tunable OFS, f_{ceo2}, m_2 and f_{beat2} are fixed at certain values while f_{rep2} is tuned precisely, via the precise laser control referenced to the frequency standard. Even though OFS2 is used for continuous tuning, its absolute frequency f_{ofs2} can be determined within the uncertainty of the optical comb by simply monitoring f_{rep2} in real time with a frequency counter.

When a THz synthesizer is realized by photomixing OFS1 and OFS2 with a photomixer, its output frequency (f_{THz}) is given by

$$\begin{aligned} f_{THz} &= \left| f_{ofs2} - f_{ofs1} \right| \\ &= \left| \left(f_{ceo2} + m_2 f_{rep2} + f_{beat2} \right) - \left(f_{ceo1} + m_1 f_{rep1} + f_{beat1} \right) \right|. \end{aligned} \quad [15.8]$$

Here, it is important to emphasize that the absolute value of f_{THz} can be determined at the uncertainty of the microwave frequency standard by measuring f_{ceo1} (fixed), f_{ceo2} (fixed), f_{rep1} (fixed), f_{rep2} (variable), m_1 (fixed), m_2 (fixed), f_{beat1} (fixed) and f_{beat2} (fixed). This is the main advantage over

traditional THz synthesizers. The continuous tuning range of f_{THz} (Δf_{THz}) is represented as:

$$\Delta f_{THz} = \Delta f_{ofs2} = m_2 \Delta f_{rep2}. \quad [15.9]$$

The value of m_2 reaches 3 880 000 when the optical frequency of CWL2 is 194 THz (corresponding wavelength = 1550 nm) and f_{rep2} is 50 MHz. For example, when Δf_{rep2} = 500 kHz, which is 1 % of f_{rep2}, Δf_{THz} could reach about 2 THz from Equation [15.9]. Therefore, the proposed method can also be used for widely and continuously tunable THz synthesizers.

15.4.2 Experimental set-up

The experimental set-up of the THz synthesizer is shown in the upper part of Fig. 15.10. We first constructed two OFSs operating at a wavelength of 1542 nm for photomixing. The fixed OFS (OFS1) was composed of a distributed feedback fiber laser (CWL1; Koheras A/S, Inc., AdjustiK E15-PM) and a custom-built optical comb including a mode-locked Er-doped fiber laser (Inaba *et al.*, 2006), namely, a fiber comb (FC1). On the other hand, the tunable OFS (OFS2) was composed of an external cavity laser diode (CWL2;

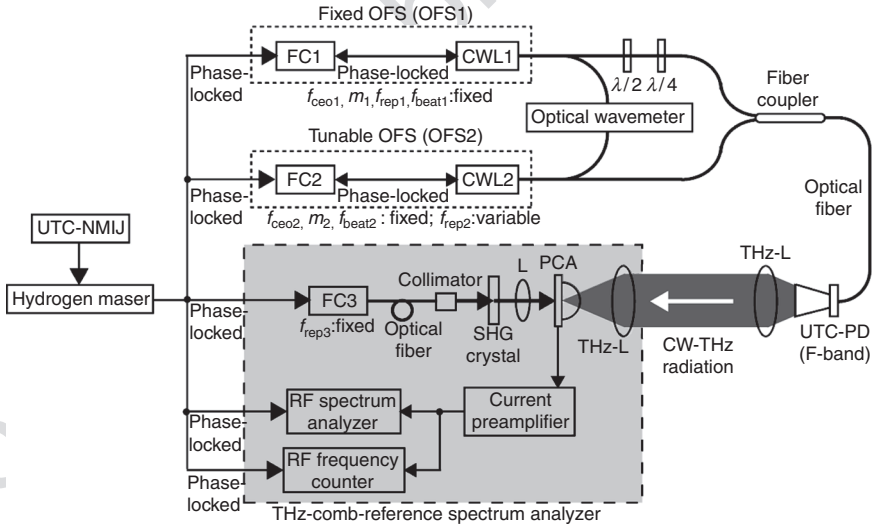

15.10 Experimental set-up. FC1, FC2 and FC3: fiber combs; CWL1 and CWL2: CW near-infrared lasers; λ/2: half-wave plate; λ/4: quarter-wave plate; UTC-PD: uni-traveling-carrier photodiode for photomixing; THz-L: THz lenses; L: lens; PCA: photoconductive antenna; SHG crystal: second-harmonic-generation crystal; UTC-NMIJ: coordinated universal time operated by the National Metrology Institute of Japan.

Optical Comb, Inc., LT-5001) and another fiber comb (FC2). The frequencies $f_{ceo1}, f_{ceo2}, f_{rep1}, f_{rep2}, f_{beat1}$ and f_{beat2} were all phase-locked to the microwave frequency reference synthesized from a hydrogen maser linked to coordinated universal time (UTC), operated by the National Metrology Institute of Japan (UTC-NMIJ). Details of the phase-locking process in the OFSs are given elsewhere (Takahashi *et al.*, 2009). The mode numbers m_1 and m_2 were selected depending upon the frequency of the generated CW-THz radiation. An optical wavemeter (Advantest Corp., Q8326) was used to determine m_1 and m_2. The continuous tuning range of Δf_{ofs2} was achieved up to 990 GHz by expanding the tuning range of CWL2 using a combination of a piezoelectric (PZT) actuator and a linear translation stage.

Promising photomixers for the THz synthesizer included a UTC-PD (Nagatsuma *et al.*, 2009) and a PCA (Matsuura *et al.*, 1997). The former had the advantages of high power characteristics and good compatibility with laser sources in the 1.5 μm telecommunication band, whereas the latter could achieve higher frequency response and broader tunability by use of 0.8 μm laser sources. Furthermore, the available frequency range in the UTC-PD could be extended to over 1 THz (Nagatsuma *et al.*, 2009). We here used an F-band UTC-PD (NTT Electronics, frequency range = 90–140 GHz) as a photomixer for actual proof of the proposed method; however, it should be emphasized that it is easily possible to use another UTC-PD or PCA in place of the F-band UTC-PD if THz synthesizers with higher frequency and/or broader tunability are required. After adjusting the polarization overlap with a half-wave plate ($\lambda/2$) and a quarter-wave plate ($\lambda/4$), the output beams from OFS1 (f_{ofs1} = 194.4 THz, power = 7.3 mW) and OFS2 (f_{ofs2} = 194.3 THz, power = 9.4 mW) were combined with a fiber coupler and then optically heterodyned with a fiber-coupled, F-band UTC-PD equipped with a horn antenna. We estimated from the observed photocurrent value (7 mA) and the set bias voltage (–2.5 V) of the UTC-PD that the average power of generated CW-THz radiations was around 250 μW in the F-band.

To evaluate the spectral characteristics of the THz synthesizer, we used a THz-comb-referenced spectrum analyzer (Yokoyama *et al.*, 2008; Yasui *et al.*, 2009) composed of a third fiber comb whose frequency f_{rep} was stabilized (FC3 with f_{rep3} = 56 122 639 Hz), a bow-tie-shaped, low-temperature-grown GaAs PCA for THz detection, and RF frequency instruments, as shown in the lower part of Fig. 15.10. The frequency f_{rep3} and RF frequency instruments were synchronized to the microwave frequency reference. The free-space-propagating CW-THz radiation passing through a pair of THz lenses (Pax Co., Tsurupica) was made incident on the PCA. The PCA was triggered by second-harmonic-generation (SHG) light (center wavelength = 775 nm, average power = 10 mW) from FC3. This resulted in the generation of the PC-THz comb of FC3 in the PCA. Photoconductive heterodyne mixing between the CW-THz radiation and the PC-THz comb in the PCA

generated beat signals in the RF region. The beat signal of the current from the PCA was amplified by a high-gain current preamplifier (bandwidth = 10 MHz, sensitivity = 105 V/A) and was measured with an RF spectrum analyzer (Agilent E4402B) and frequency counter (Agilent 53132A). Details of the THz-comb-referenced spectrum analyzer are given in Section 15.3. The spectral behavior and frequency instability of the CW-THz radiation were measured with the THz-comb-referenced spectrum analyzer. On the other hand, the absolute frequency of the CW-THz radiation was determined based on Equation [15.8].

15.4.3 Results

To evaluate the spectral characteristics in the THz synthesizer, we first generated frequency-locked CW-THz radiation at upper and lower frequency limits within the F-band, ranging from 90 GHz to 140 GHz. Figures 15.11a and b show spectra of the beat signal for CW-THz radiation around 91.97 GHz and 140.0 GHz, respectively. The lower horizontal axes gave the frequency scale (f_{beat3}) measured with the RF spectrum analyzer. One can clearly confirm that the CW-THz radiation spectra have similar Gaussian-like shapes at these two frequencies. The linewidth of the CW-THz radiation was 599 kHz at 91.97 GHz and 631 kHz at 140.0 GHz when a Gaussian function was fitted to the spectral shape by regression analysis based on the Levenberg–Marquardt algorithm. If a combination of narrower-linewidth CW lasers with fast feedback control is employed for the OFSs, the linewidth of the CW-THz radiation will be further decreased.

We next assigned an absolute frequency to each CW-THz spectrum in Fig. 15.11. In the THz-comb-referenced spectrum analyzer, the absolute frequency of the CW-THz radiation (f_{THz}) is given by Equations [15.3a] or [15.3b]. When the CW-THz radiation had sufficiently narrow linewidth, its absolute frequency was determined at an uncertainty of 10–11 as described in Section 15.3. However, when the linewidth of the CW-THz radiation became broader, around 1 MHz, fitting analysis of the beat signal spectrum to determine its center frequency included an error of a few kHz (Yasui *et al.*, 2010b; Yasui *et al.*, 2011b). This resulted in an uncertainty of 10^{-3} in the absolute frequency measurement even though the actual frequency of the CW-THz radiation was more stable and accurate. Conversely, if all parameters in Equations [15.6] and [15.7] are known, the absolute frequency of the CW-THz radiation can be simply determined from Equation [21.8] without the need for the THz-comb-reference spectrum analyzer. Therefore, we decided to determine the absolute frequency using Equation [15.8]. Parameters of OFS1 and OFS2 are summarized in Tables 15.1 and 15.2 when f_{THz} = 91.97 GHz and 140.0 GHz in Fig. 15.11. From these values, center frequencies for those two CW-THz radiation spectra were 91 974 517 201 Hz and 140 003 403 918 Hz, respectively. The upper horizontal axes

Table 15.1 Parameters of OFS1 and OFS2 when f_{THz} = 91 974 517 201 Hz

	f_{ceo} (Hz)	m	f_{rep} (Hz)	f_{beat} (Hz)	f_{ofs} (Hz)
OFS1	10 683 000	3 889 263	49 985 122.0	–21 384 000	194 405 274 844 086
OFS2	10 683 000	3 812 171	50 971 800.5	69 960 000	194 313 300 326 885

Table 15.2 Parameters of OFS1 and OFS2 when f_{THz} = 140 003 403 918 Hz

	f_{ceo} (Hz)	m	f_{rep} (Hz)	f_{beat} (Hz)	f_{ofs} (Hz)
OFS1	10 683 000	3 889 264	49 985 129.0	–21 384 000	194 405 352 054 056
OFS2	10 683 000	3 811 224	50 971 884.1	69 960 000	194 265 348 650 138

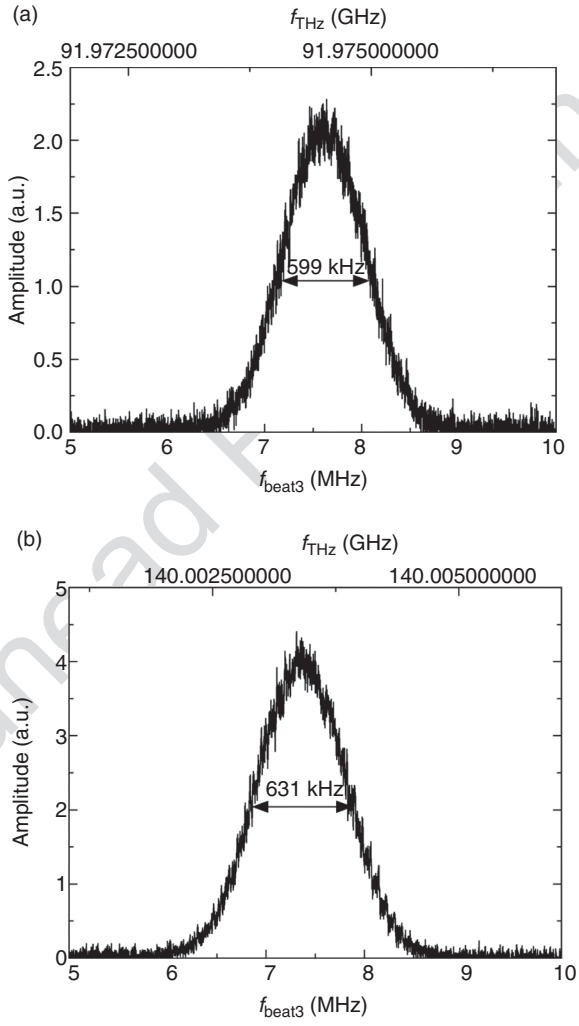

15.11 Spectra of CW-THz radiation at (1) 91.97 GHz and (b) 140.0 GHz.

in Fig. 15.11a and b show the actual scale of the absolute frequency determined by Equation [15.8]. Here, it is important to note that their absolute frequency is traceable to the hydrogen maser because two OFSs are fully phase-locked to the maser and the phase-noise in photomixer is negligible.

We also evaluated the frequency instability of the CW-THz radiation set at 132.0 GHz by measuring the frequency fluctuation of the beat signal (f_{beat3}) with the RF frequency counter. Figure 15.12 shows the fluctuation of the beat frequency, represented by the Allan standard deviation σ_A (Allan, 1966), with respect to various averaging times τ. A power law relationship in the form $\sigma_A = \tau^{-1}$ between averaging time τ and frequency fluctuation σ_A was found. The inverse proportionality between them clearly indicates that the output frequency of the THz synthesizer was phased-locked to the hydrogen maser. Here, we consider whether the frequency fluctuation of the THz synthesizer is consistent with that of the OFS. The THz synthesizer had a frequency fluctuation of about 10 kHz at an averaging time of 1 s (see Fig. 15.12). Conversely, since the frequency uncertainties of f_{ceo1} (or f_{ceo2}), f_{rep1} (or f_{rep2}) and f_{beat1} (or f_{beat2}) in OFS1 (or OFS2) were respectively 10–17, 10–12 and 10–13 at an averaging time of 1 s (Takahashi *et al.*, 2009), the frequency fluctuation in the OFS was estimated to be a few hundreds of Hz from the uncertainty of $m_1 f_{rep1}$ (or $m_2 f_{rep2}$), which is mainly due to the uncertainty of the frequency synthesis of f_{rep1} (or f_{rep2}). We consider that the discrepancy of frequency fluctuation between THz and optical synthesizers is mainly due to electrical noise caused in the amplification processes of the considerably weak beat signal in the THz-comb-referenced spectrum analyzer.

AQ3

Next, we show the result of incremental tuning of the CW-THz radiation around 133 GHz by scanning f_{rep2} at 0.2 Hz intervals. The resulting consecutive spectra of the CW-THz radiation are shown in Fig. 15.13 (sweep time = 2.483 s, RBW = 10 kHz, number of integrated signals = 50), in which the horizontal coordinate is scaled by Equation [15.8]. It is important to note that a tiny increment of 0.2 Hz in f_{rep2} caused a large change of 762 281.6 Hz in f_{THz} due to a large tuning rate in Equation [15.9] (m_2 = 3 811 408 in this demonstration). This tuning rate is three orders of magnitude larger than that of the previous THz synthesizer using the single comb (Quraishi *et al.*, 2005).

Finally, we demonstrated continuous tuning of the CW-THz radiation over 1 GHz. The initial value of f_{THz} was set at 131.71 GHz. Figure 15.14a shows the display on the RF spectrum analyzer before starting tuning; here, the frequency span of the RF spectrum analyzer was set to be 60 MHz. Two beat signals between the CW-THz radiation and PC-THz comb were confirmed at 7.4 MHz and 48.7 MHz. Conversely, a signal around 56.1 MHz arose from self-beating of FC3 with f_{rep3} of 56 122 639 Hz, used for the THz-comb-reference spectrum analyzer. Frequency dependence of the gain and the noise characteristics in the current preamplifier used in the THz

AQ4

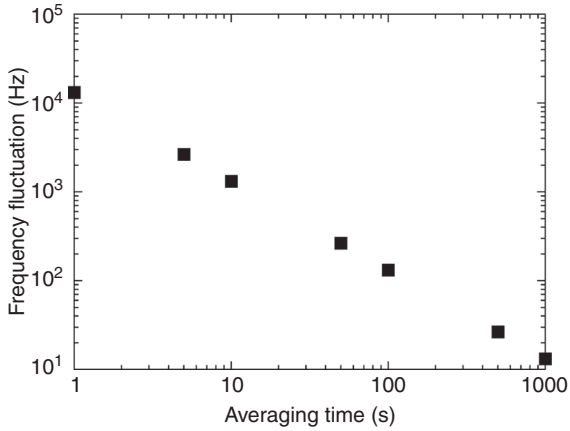

15.12 Frequency fluctuation of CW-THz radiation at 132.0 GHz with respect to averaging time.

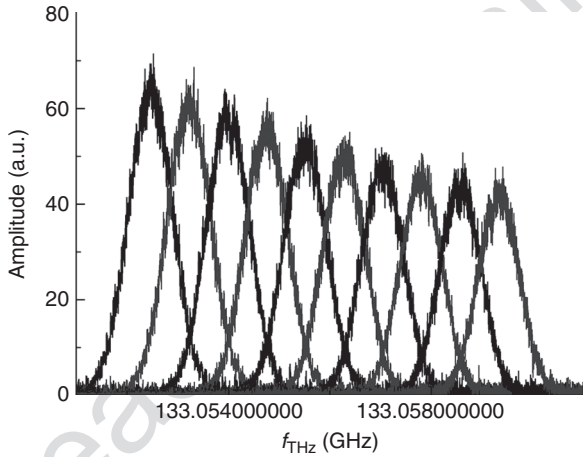

15.13 Incremental tuning of CW-THz radiation around 133 GHz when scanning f_{rep2} at 0.2 Hz intervals.

spectrum analyzer cause the power difference between the two beat signals and the raised background floor, respectively. The spectral configuration of the CW-THz radiation and PC-THz comb before tuning is illustrated in the upper part of Fig. 15.14b. The mode number m_{THz} of the PC-THz comb mode nearest in frequency to the CW-THz radiation was estimated to be 2347 from f_{THz} and f_{rep3}. Then, the f_{THz} value was continuously tuned to 132.97 GHz for 60 s by scanning f_{rep2}. Since m_{THz} after tuning was 2369, as illustrated

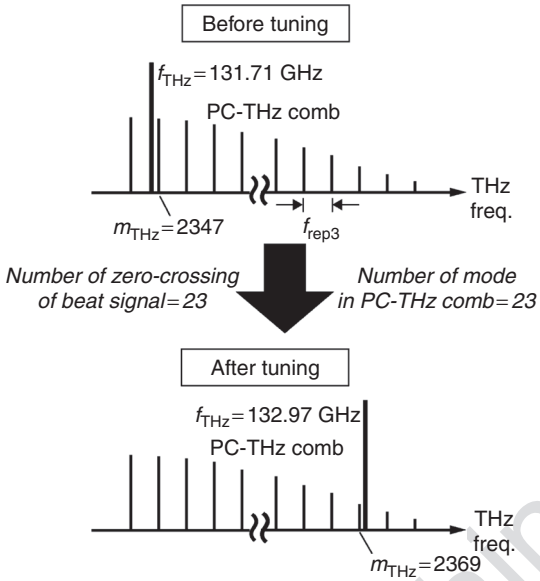

15.14 Spectral configuration of CW-THz radiation and PC-THz comb before and after tuning.

in the lower part of Fig. 15.14b, the CW-THz radiation traverses the PC-THz comb modes at 23 points. The actual spectral behavior of the beat signals during continuous tuning is shown as a video elsewhere (Yasui *et al.*, 2011b). It was confirmed that two beat signals appeared and disappeared one after another. The beat signal at the lower frequency was generated by mixing the CW-THz radiation with the mode number m_{THz} of PC-THz comb nearest in frequency, whereas the beat signal at the higher frequency was due to mixing with m_{THz+1} or m_{THz-1}. Since zero crossing of the beat signal means that the CW-THz radiation traverses the PC-THz comb mode, scanning of f_{THz} by 1.26 GHz should cause zero crossing of the beat signal 23 times. The actual number of zero crossings was 23, which was exactly the same as the expected number. In this way, we confirmed from both Equation [15.8] and THz spectrum analyzer that the continuous tuning of 1.26 GHz was surely performed. This continuous tuning range can be extended to the full frequency bandwidth of the F-band UTC-PD photomixer because we also generated CW-THz radiation at the lower limit (91.97 GHz) and the upper limit (140.0 GHz) of frequency in the F-band (see Fig. 15.11). We believe that it should be possible to further extend the tuning range to 990 GHz in the THz frequency region by use of a broadband photomixer, such as a PCA (Matsuura *et al.*, 1997), because we have already achieved continuous tuning of 990 GHz in the tunable OFS.

15.5 THz-comb-referenced spectrometer

THz-TDS is a popular spectroscopic technique for obtaining a broadband THz spectrum. In this method, marking of a frequency scale in the THz spectrum is performed by a mechanical scanning time delay with a motor-driven translation stage. However, poor positioning precision and limited stroke length of the translation stage hinder the achievement of high spectral resolution and accuracy in THz-TDS. This sometimes leads to inconsistency of frequency scales in the THz spectrum among different THz-TDS systems. On the other hand, THz frequency domain spectroscopy (THz-FDS) with a tunable narrow-linewidth CW-THz wave is a promising spectroscopic technique to achieve high spectral resolution. Unfortunately, the spectral range covered by this method is much narrower than that in THz-TDS. The accuracy of the frequency scale in this method depends on the performance of an optical wavemeter for measuring the wavelengths of two CW near-infrared lasers for photomixing, which is typically 10^{-6} to 10^{-7}. In this way, the conventional spectroscopic techniques have both merits and demerits. If we could only combine the merits of both THz-TDS and THz-FDS, and also mark the frequency scale of the spectrum accurately based on a frequency standard, the ultimate THz spectrometer with high accuracy, high resolution, and a broad spectral range would be achieved. Coherent linking of frequency with a frequency comb, described in Section 15.2, has the potential to achieve this ultimate THz spectrometer, because the THz comb has both characteristics of CW-THz waves and a broadband THz spectrum, and the absolute frequencies of all comb modes are traceable to the microwave frequency standard. To realize this concept, we developed a multi-frequency-heterodyning THz-comb-referenced spectrometer (Yasui *et al.*, 2006; Yasui *et al.*, 2010a).

15.5.1 Principle of operation

Let us consider THz generation from a PCA emitter excited by a femtosecond laser (pump laser; mode-locked frequency f_{rep1}) and THz detection using a PCA detector gated by another femtosecond laser (probe laser; mode-locked freq. = f_{rep2}). Figure 15.15 illustrates spectral behaviors in (a) optical, (b) THz and (c) RF regions. In the frequency domain, since the PCA generation of the THz pulse can be considered as an ultra-wideband demodulation of an optical frequency comb, the optical comb is down-converted to the THz region without any change to the frequency spacing. The resulting THz comb of electromagnetic wave, namely EM-THz comb, is a harmonic frequency comb without a frequency offset, composed of a fundamental component (freq. = f_{rep1}) and a series of harmonic components (freq. = $2f_{rep1}$, $3f_{rep1}$, …, nf_{rep1}) of a mode-locked frequency. Next, we consider what happens when the mode-locked frequency of the probe laser

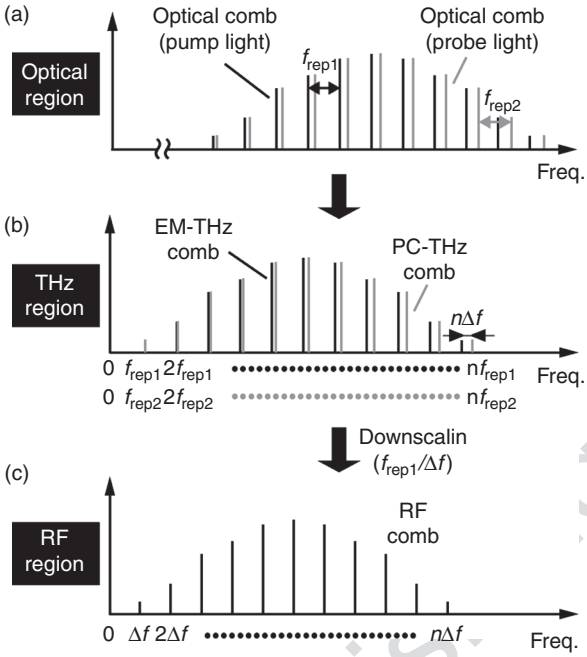

15.15 Spectral behavior of frequency combs in (a) optical, (b) THz, and (c) RF regions.

($f_{rep2} = f_{rep1} + \Delta f$) is slightly detuned from that of the pump laser (f_{rep1}) by a certain frequency offset (Δf). Instantaneous photoconductive gating by the probe laser induces a frequency comb of photocarrier, namely PC-THz comb, having a different frequency spacing (freq. = f_{rep2}, $2f_{rep2}$, $3f_{rep2}$, …, nf_{rep2} = ($f_{rep1} + \Delta f$), $2(f_{rep1} + \Delta f)$, $3(f_{rep1} + \Delta f)$, …, $n(f_{rep1} + \Delta f)$) in the PCA detector, which is also existed in THz frequency region. Under this condition, it is possible to detect the EM-THz comb as a result of the photoconductive process occurring between the EM-THz and PC-THz combs, giving rise to the multi-frequency-heterodyning effect. This results in the generation of a secondary frequency comb in the RF region, termed the RF comb (freq. = Δf, $2\Delta f$, $3\Delta f$, …, $n\Delta f$). Since the RF comb is a replica of the EM-THz comb only downscaled by $f_{rep1}/\Delta f$ in frequency, one can utilize the THz comb easily via direct observation of the RF comb using an RF spectrum analyzer and calibration of the frequency scale.

15.5.2 Experimental set-up

Figure 15.16 shows a schematic diagram of the experimental set-up. We constructed two self-starting, stretched-pulse mode-locked, Er-fiber lasers

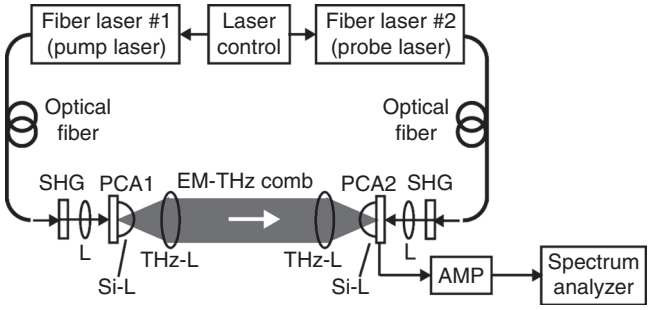

15.16 Experimental set-up. SHG: second-harmonic-generation crystal; L: lenses; PCA1 and PCA2: dipole-shaped LTG-GaAs photoconductive antennas; Si-L: hemispherical silicon lenses; THz-L: THz lenses; AMP: current preamplifier.

(center wavelength = 1550 nm, pulse duration = 50 fs and mean power = 90 mW) (Inaba *et al.*, 2006) for use as laser sources (pump and probe lasers) to generate and detect EM-THz comb. The individual mode-locked frequencies of the two lasers (f_{rep1} = 56 124 000 Hz and f_{rep2} = 56 124 005 Hz) and the frequency difference between them ($\Delta f = f_{rep2} - f_{rep1}$ = 5 Hz) were stabilized by two independent PI (proportional and integral) control systems with reference to a rubidium (Rb) frequency standard (accuracy = 5×10^{-11}, instability = 2×10^{-11} at 1 s). The instability of the mode-locked frequency was equal to that of the Rb frequency standard whereas the timing jitter between the two lasers was less than 300 fs. Excellent stability of f_{rep1}, f_{rep2} and Δf enables generating stable frequency combs and achieving an exact multi-frequency-heterodyning process. Output light from the pump laser was delivered by an optical fiber and was converted by SHG to half its original wavelength using an SHG crystal (β-BaB_2O_4). The resulting 775-nm SHG light was focused on the gap of a dipole-shaped low-temperature-grown GaAs (LTG-GaAs) PCA for THz generation (PCA1; length = 7.5 μm, width = 10 μm, gap = 5 μm). The EM-THz comb from PCA1 propagated in free space through two pairs of hemispherical silicon lenses (Si-L) and THz lenses (THz-L), and was then incident on another dipole-shaped LTG-GaAs PCA (PCA2) gated by the SHG light of the probe laser, which had the PC-THz comb. A fully fiber-coupled THz spectrometer would be achieved without the need for frequency doubling if a PCA for a 1550 nm light were used (Sartorius *et al.*, 2008). As a result of multi-frequency-heterodyning photoconductive detection, the RF comb was directly measured with an RF spectrum analyzer (Agilent Technologies, E4402B) after passing through a high-gain current preamplifier (AMP). One can reconstruct the EM-THz comb exactly by calibrating the RF comb with the frequency downscale factor (= $f_{rep1}/\Delta f$ = 11 224 800).

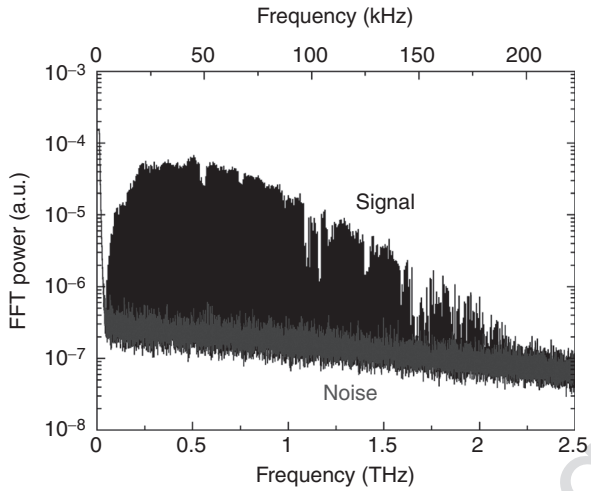

15.17 Power spectrum of EM-THz comb.

15.5.3 Results

Figure 15.17 shows a power spectrum of the RF comb obtained using the proposed method (measurement time = 100 s), in which the upper horizontal axis gives the frequency scale in the RF spectrum analyzer. One can confirm that the RF comb is distributed within a frequency range of 200 kHz. The actual frequency values in the THz comb spectrum are scaled according to the lower horizontal axis by using the frequency downscale factor. The tail of the observed spectrum was achieved to 2 THz. The spectrum painted over is actually composed of a series of frequency spikes regularly separated by the mode-locked frequency. Considering a spectral range of 2 THz and a frequency spacing of 56.1 MHz, the THz spectrum is composed of over 35 000 comb modes. Several absorption lines caused by atmospheric water vapor were clearly observed as dips in the spectrum of Fig. 15.17.

To confirm the validity of the observed spectrum, we also measured the power spectrum of the pulsed THz radiation at the same experimental condition using asynchronous-optical-sampling THz-TDS (ASOPS-THz-TDS) (Yasui *et al.*, 2005, 2010a). In the case of the ASOPS-THz-TDS, the signal of THz radiation was measured in time domain using a fast digitizer triggered by a sum-frequency-generation cross-correlation signal (not shown in Fig. 15.16), in place of the RF spectrum analyzer. Figure 15.18 shows the power spectrum of the THz radiation and the noise, in which signal averaging of 500-sweep sequences was carried out by the digitizer. Spectral shape and bandwidth in Fig. 15.17 was almost equal to those in Fig. 15.18. The reason for difference of dynamic range in power is mainly due to a difference in

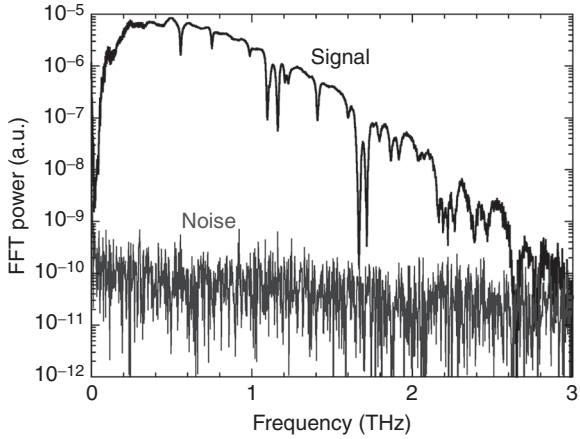

15.18 Power spectrum of THz radiation measured by ASOPS-THz-TDS.

efficiency of signal acquisition between the spectrum analyzer and the digitizer. Detail discussion on this point is given elsewhere (Yasui *et al.*, 2010a).

15.6 Conclusions and future trends

We described the concept of THz frequency metrology based on a frequency comb, together with three concrete techniques embodying this concept. The most important point in our approach is that the coherent linking of the frequency established by the frequency comb enables us to realize THz frequency metrology traceable to the SI base unit of time. Also, the fiber-based techniques used here, including fiber lasers and optical fibers, have the advantage of being portable, alignment-free, robust and flexible. First, the THz-comb-referenced spectrum analyzer was achieved by photoconductive mixing of a CW-THz wave with a PC-THz comb. Based on the stable PC-THz comb generated in a PCA, the absolute frequency of the CW-THz wave was determined at a precision of 10^{-11}, which is limited by the performance of the Rb atomic clock used. Furthermore, the detailed spectral behavior of the CW-THz waves was monitored in real time. Second, a widely and continuously tunable THz synthesizer traceable to the hydrogen maser linked to UTC-NMIJ was demonstrated by photomixing of two independent OFSs. A combination of dual optical combs and the photomixing technique achieved a frequency uncertainty of 10–12 in the THz frequency range. Furthermore, photomixing of a tunable OFS and a fixed one enabled us to extend the continuous tuning range of the CW-THz radiation up to 1.26 GHz while maintaining unprecedented frequency uncertainty. Third, a THz-comb-referenced spectrometer traceable to the microwave frequency

standard was constructed using dual THz combs. The EM-THz comb was downscaled to the RF region by using a multi-frequency-heterodyning technique and was then measured directly with an RF spectrum analyzer. Frequency modes constituting the THz comb will be used as frequency markers, having an interval of 56 MHz, for a broadband THz spectrum.

Our approach for THz frequency metrology enables us to treat the frequency in the THz region as a universal quantity based on the national frequency standard, in the same manner as in the optical and electrical regions. Therefore, the so-called THz gap problem will be essentially solved. Establishment of THz frequency metrology will cause a ripple effect in various fields of THz technology and applications. For example, to achieve universal identification power in spectroscopic applications, uncertainty of the frequency scale in the THz spectrum should be certified by referencing to the SI base unit of time, that is, a microwave frequency standard. Our THz frequency metrology will play an important role in frequency calibration and traceability of various types of commercial THz instruments, such as sources, detectors and systems. The absolute frequency of CW-THz sources can be accurately determined by THz spectrum analyzers, whereas the frequency scale of a THz spectrometer can be precisely calibrated by THz synthesizers. The precisely calibrated THz spectrometer will increase the identification power in spectroscopic applications based on THz spectral fingerprints. Also, the highly spectroscopic performance made possible by using a THz comb will contribute to the development of precise THz spectrometers and preparation of a precise spectral database atlas. Furthermore, when THz waves are used as carrier waves for broadband wireless communications, the transmission frequency should be highly accurate and stable in order to secure the necessary and sufficient bandwidth for broadband communication without interference with other applications, such as astronomy or sensing. A THz synthesizer can be used to generate an accurate and stable transmission frequency. In this way, THz frequency metrology will spread to various THz applications based on a high-reliability frequency scale.

15.7 References

Allan DW (1966), 'Statistics of atomic frequency standards', *Proc. IEEE*, **54**, 221–230.

Baselmans JJA, Hajenius M, Gao JR, Klapwijk TM, de Korte PAJ, Voronov B, and Gol'tsman G (2004), 'Doubling of sensitivity and bandwidth in phonon cooled hot electron bolometer mixers', *Appl. Phys. Lett.*, **84**, 1958–1960.

Champenois C, Hagel G, Houssin M, Knoop M, Zumsteg C, and Vedel F (2007), 'Terahertz frequency standard based on three-photon coherent population trapping', *Phys. Rev. Lett.*, **99**, 013001.

Gaal P, Raschke MB, Reimann K, and Woerner M (2007), 'Measuring optical frequencies in the 0–40 THz range with non-synchronized electro–optic sampling', *Nature Photon.*, **1**, 577–580.

Gopalakrishnan GK, Burns WK, and Bulmer CH (1993), 'Microwave-optical mixing in $LiNbO_3$ modulators', *IEEE Trans. Microwave Theory and Techniques*, **41**, 2383–2391.

Inaba H, Daimon Y, Hong F-L, Onae A, Minoshima K, Schibli TR, Matsumoto H, Hirano M, Okuno T, Onishi M, and Nakazawa M (2006), 'Long-term measurement of optical frequencies using a simple, robust and low-noise fiber based frequency comb', *Opt. Express*, **14**, 5223–5231.

Katayama I, Akai R, Bito M, Shimosato H, Miyamoto K, Ito H, and Ashida M (2010), 'Ultrabroadband terahertz generation using 4-N,N-dimethylamino-4 -N -methyl-stilbazolium tosylate single crystals', *Appl. Phys. Lett.*, **97**, 021105.

Kleine-Ostmann T, Schrader T, Bieler M, Siegner U, Monte C, Gutschwager B, Hollandt J, Müller R, Ulm G, Pupeza I, and Koch M (2008), 'THz metrology', *Frequenz*, **62**, 135–146.

Kohjiro S, Kikuchi K, Maezawa M, Furuta T, Wakatsuki A, Ito H, Shimizu N, Nagatsuma T, and Kado Y (2008), 'A 0.2–0.5 THz single-band heterodyne receiver based on a photonic local oscillator and a superconductor-insulator-su perconductor mixer', *Appl. Phys. Lett.*, **93**, 093508.

Kolner BH and Bloom DM (1986), 'Electro-optic sampling in GaAs integrated circuits', *IEEE J. Quantum Electron.*, **22**, 79–93.

Matsuura S, Tani M, and Sakai K (1997), 'Generation of coherent terahertz radiation by photomixing in dipole photoconductive antennas', *Appl. Phys. Lett.*, **70**, 559–561.

Mittleman DM (2003), *Sensing with THz radiation*, Berlin, Springer.

Nagatsuma T, Ito H, and Ishibashi T (2009), 'High-power RF photodiodes and their applications', *Laser Photon. Rev.*, **3**, 123–137.

Quraishi Q, Griebel M, Kleine-Ostmann T, and Bratschitsch R (2005), 'Generation of phase-locked and tunable continuous-wave radiation in the terahertz regime', *Opt. Lett.*, **30**, 3231–3233.

Sartorius B, Roehle H, Künzel H, Böttcher J, Schlak M, Stanze D, Venghaus H, and Schell M (2008), 'All-fiber terahertz time-domain spectrometer operating at 1.5 μm telecom wavelengths', *Opt. Express*, **16**, 9565–9570.

Schnatz H, Lipphardt B, Helmcke J, Riehle F, and Zinner G (1996), 'First phase-coherent frequency measurement of visible radiation', *Phys. Rev. Lett.*, **76**, 18–21.

Takahashi H, Nakajima Y, Inaba H, and Minoshima K (2009), 'Ultra-broad absolute-frequency tunable light source locked to a fiber-based frequency comb', Technical Digest of *Conference on Lasers and Electro-Optics 2009*, Optical Society of America, Washington DC, paper CTuK4.

Tonouchi M (2007), 'Cutting-edge terahertz technology', *Nature Photon.,* **1**, 97–105.

Udem Th, Holzwarth R, and Hänsch TW (2002), 'Optical frequency metrology', *Nature*, **416**, 233–237.

Yasui T, Saneyoshi E, and Araki T (2005), 'Asynchronous optical sampling terahertz time-domain spectroscopy for ultrahigh spectral resolution and rapid data acquisition', *Appl. Phys. Lett.*, **87**, 061101.

Yasui T, Kabetani Y, Saneyoshi E, Yokoyama S, and Araki T (2006), 'Terahertz frequency comb by multi-frequency-heterodyning photoconductive detection for high-accuracy, high-resolution terahertz spectroscopy', *Appl. Phys. Lett.*, **88**, 241104.

Yasui T, Nakamura R, Kawamoto K, Ihara A, Fujimoto Y, Yokoyama S, Inaba H, Minoshima K, Nagatsuma T, and Araki T (2009), 'Real-time monitoring of continuous-wave terahertz radiation using a fiber-based, terahertz-comb-referenced spectrum analyzer', *Opt. Express*, **17**, 17034–17043.

Yasui T, Nose M, Ihara A, Kawamoto K, Yokoyama S, Inaba H, Minoshima K, and Araki T (2010), 'Fiber-based, hybrid terahertz spectrometer using dual fiber combs', *Opt. Lett.*, **35**, 1689–1691.

Yasui T, Takahashi H, Iwamoto Y, Inaba H, and Minoshima K (2010), 'Continuously tunable, phase-locked, continuous-wave terahertz generator based on photomixing of two continuous-wave lasers locked to two independent optical combs', *J. Appl. Phys.*, **107**, 033111.

Yasui T, Yokoyama S, Inaba H, Minoshima K, Nagatsuma T, and Araki T (2011), 'Terahertz frequency metrology based on frequency comb', *IEEE J. Selected Topics in Quantum Electron.*, **17**, 191–201.

Yasui T, Takahashi H, Kawamoto K, Iwamoto Y, Arai K, Araki T, Inaba H, and Minoshima K (2011), 'Widely and continuously tunable terahertz synthesizer traceable to a microwave frequency standard', *Opt. Express*, **19**, 4428–4437.

Yokoyama S, Nakamura R, Nose M, Araki T, and Yasui T (2008), 'Terahertz spectrum analyzer based on a terahertz frequency comb', *Opt. Express*, **16**, 13052–13061.

AU1:	Please check the citation 'Kolner et al., 1986' changed to 'Kolner and Bloom, 1986'.
AQ2:	We have changed 5.6 x 10 -12 to 5.6 × 10–12. Is this okay?
AQ3:	Should this be: 10–17, 10–12 and 10–13 ?
AQ4:	As per the publisher's instruction, we have deleted Fig. 15.14a. Therefore, please confirm whether the sentence 'Figure 15.14a shows the display…' can be deleted. Also, please clarify whether any other changes need to be made to the text.